Journal of Sound and Vibration (1999) **228**(5), 1035–1056
Article No. jsvi.1999.2456, available online at http://www.idealibrary.com on IDEAL®

DYNAMIC ANALYSIS OF AN AUTOMATIC DYNAMIC BALANCER FOR ROTATING MECHANISMS

J. CHUNG

Department of Mechanical Engineering, Hanyang University, 1271 *Sa*-1-*dong*, *Ansan*, *Kyunggi-do* 425-791, *Korea*

AND

D. S. RO

ROM R&D Group, ROM Business Team, Samsung Electronics Co., Ltd, 416 *Maetan*-3-*dong*, *Paldal-Gu, Suwon City, Kyunggi-do* 442-742, *Korea*

(*Received* 24 *September* 1998, *and in final form* 11 *June* 1999)

Dynamic stability and behavior of an automatic dynamic balance (ADB) are analyzed by a theoretical approach. Using Lagrange's equation, we derive the non-linear equations of motion for an autonomous system with respect to the polar co-ordinate system. From the equations of motion for the autonomous system, the equilibrium positions and the linear variational equations are obtained by the perturbation method. Based on the variational equations, the dynamic stability of the system in the neighborhood of the equilibrium positions is investigated by the Routh–Hurwitz criteria. The results of the stability analysis provide the design requirements for the ADB to achieve balancing of the system. In addition, in order to verify the stability of the system, time responses are computed by the generalized-α method. We also investigate the dynamic behavior of the system and the effects of damping on balancing.

1. INTRODUCTION

Unbalance in rotating machines is a common source of vibration excitation. Many efforts have been focused on reducing unbalance. When a rotor has a fixed amount of unbalance, only one time of balancing is sufficient. However, if the unbalance is varied depending on operating conditions, the unbalance cannot be eliminated by only once. An automatic dynamic balancer (ADB) is a device to automatically eliminate the variable unbalance of rotating mechanisms. The ADB may have many applications, e.g., CD-ROM or DVD drives, washing machines and machining tools.

Although the ADB has many application areas and many patents were granted for various types of the ADB, not many studies have been performed on them. An ADB was theoretically analyzed by Alexander [1] who did not show why it worked. Cade [2] suggested the requirements of an ADB, but he did not explain the

0022-460X/99/501035 + 22 $30.00/0

theoretical background of his suggestion clearly. Recently, Lee [3] and Lee and Van Moorhem [4] presented theoretical and experimental analyses of an ADB. They showed that the ADB could balance a rotating system when the system operated above the critical speed. However, they did not explain why the ADB could not balance the system in some cases even when it operated above the critical speed. In other words, their presentation did not provide the explicit requirements for the ADB to balance the system. Since they derived the equations of motion with the rectangular co-ordinate system, the equations are for a non-autonomous system that requires the application of the Floquet theory to stability analysis. The application of the Floquet theory may be cumbersome and may need a lot of computation time; hence, it may yield inaccurate stability results. For this reason, their studies have limitations on the complete stability analysis.

In this paper, we analyze the stability and dynamic behavior of an ADB. The non-linear equations of motion for the Jeffcott rotor with the ADB are derived with the polar co-ordinate system, which makes it possible to express the equations of motion as those for an autonomous system. From the equations for the autonomous system, the equilibrium positions and the linear variational equations are derived by the perturbation method. Using the Routh–Hurwitz criteria, the stability of the system is analysed in the neighborhood of the equilibrium positions that may be divided into the balanced and unbalanced positions. The stability analysis furnishes the design requirements for the ADB to achieve balancing of the system. In addition, the time responses of the system are computed by the generalized-α method [5]. From the response analysis, we verify the results of the stability analysis and we also demonstrate the effects of the fluid damping and the damping factor on the balancing of the system.

2. NON-LINEAR EQUATIONS OF MOTION

The whirling Jeffcott rotor with the ADB is shown in Figure 1 where a disk is symmetrically located on a shaft supported by two bearings. The centre of mass of the disk is at G and the centerline of the bearings intersects the plane of the disk at O. The ADB is composed of a circular disk with a groove containing balls and a damping fluid. The balls move freely in the groove and the disk rotates with angular velocity ω. As shown in Figure 2, the centroid C is defined by the polar co-ordinates r and θ, while the center of mass G is defined by eccentricity ε and angle ωt for the given position of the centroid. The angular positions of the balls are given by the pitch radius R and angle ϕ_i for $i = 1, \ldots, n$ (n is the total number of the balls in the groove).

The non-linear equations of motion for the ADB are derived from Lagrange's equation given by

$$\frac{\mathrm{d}}{\mathrm{d}t}\left(\frac{\partial T}{\partial \dot{q}_k}\right) - \frac{\partial T}{\partial q_k} + \frac{\partial V}{\partial q_k} + \frac{\partial F}{\partial \dot{q}_k} = 0, \tag{1}$$

where T is the kinetic energy, V is the potential energy, F is Rayleigh's dissipation function, and q_k are the generalized co-ordinates. For the given system, the

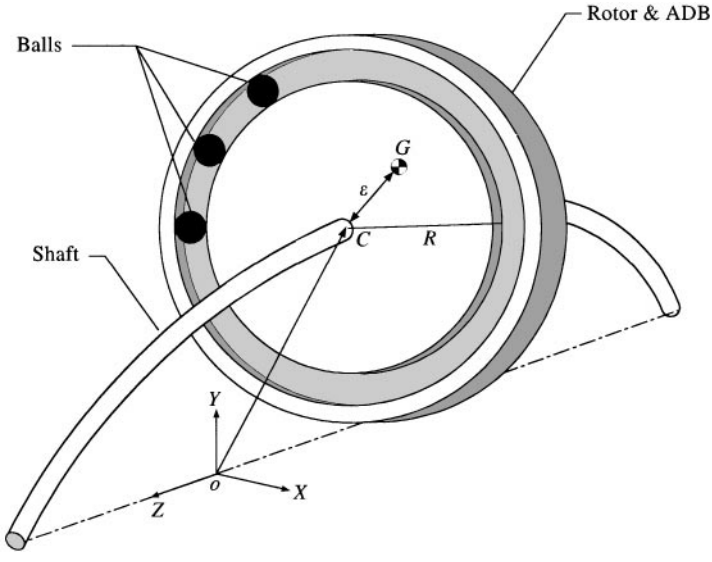

Figure 1. Jeffcott rotor with the automatic dynamic balancer.

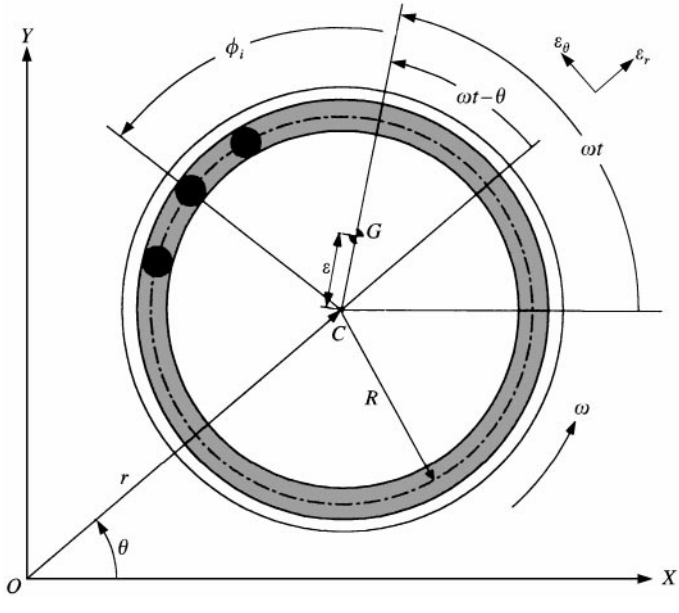

Figure 2. Configuration of the automatic dynamic balancer.

generalized co-ordinates are r, θ and ϕ_i $(i = 1, \ldots, n)$; therefore, the dynamic behavior is governed by $n + 2$ independent equations of motion.

The kinetic energy, potential energy and Rayleigh's dissipation function are needed to derive the equations of motion. Assuming that the disk moves only in the XY plane, the position vector of the centre of mass G is expressed as

$$\mathbf{r}_G = [r + \varepsilon \cos(\omega t - \theta)]\ \mathbf{e}_r + \varepsilon \sin(\omega t - \theta)\ \mathbf{e}_\theta, \tag{2}$$

and the position vector of the ith ball is given by

$$\mathbf{r}_{Bi} = [r + R\cos(\phi_i + \omega t - \theta)]\,\mathbf{e}_r + R\sin(\phi_i + \omega t - \theta)\,\mathbf{e}_\theta, \quad i = 1, 2, \ldots, n, \tag{3}$$

where $\mathbf{e}_r$ and $\mathbf{e}_\theta$ are the unit vectors in the r and θ directions respectively. Assuming that the balls have small radii and equal mass, the kinetic energy of the ADB is given by

$$T = \tfrac{1}{2} I_G \omega^2 + \tfrac{1}{2} M \dot{\mathbf{r}}_G \cdot \dot{\mathbf{r}}_G + \tfrac{1}{2} m \sum_{i=1}^{n} \dot{\mathbf{r}}_{Bi} \cdot \dot{\mathbf{r}}_{Bi}, \tag{4}$$

where I_G is the mass moment of inertia of the disk with respect to G, M is the mass of the disk, and m is the mass of a ball. Substitution of equations (2) and (3) into equation (4) yields

$$\begin{aligned} T = {} & \tfrac{1}{2}(I_G + M\varepsilon^2)\omega^2 + \tfrac{1}{2}(M + nm)(\dot{r}^2 + r^2\dot{\theta}^2) - M\varepsilon\omega[\dot{r}\sin(\omega t - \theta) - r\dot{\theta}\cos(\omega t - \theta)] \\ & + m\sum_{i=1}^{n}\{\tfrac{1}{2} R^2(\dot{\phi}_i + \omega)^2 - R(\dot{\phi}_i + \omega)[\dot{r}\sin(\phi_i + \omega t - \theta) \\ & - r\dot{\theta}\cos(\phi_i + \omega t - \theta)]\}. \end{aligned} \tag{5}$$

Neglecting gravity, the potential energy can be expressed as

$$V = \tfrac{1}{2} k r^2, \tag{6}$$

where k is the equivalent stiffness of the rotor system. On the other hand, Rayleigh's dissipation function is given by

$$F = \tfrac{1}{2} c(\dot{r}^2 + r^2\dot{\theta}^2) + \tfrac{1}{2} D \sum_{i=1}^{n} \dot{\phi}_i^2, \tag{7}$$

where c is the equivalent damping coefficient and D is the viscous drag coefficient. It is assumed that the balls have the same viscous drag coefficient D.

The non-linear equations of motion are obtained by substituting equations (5)–(7) into equation (1):

$$\begin{aligned} & (M + nm)(\ddot{r} - r\dot{\theta}^2) + c\dot{r} + kr - mR\sum_{i=1}^{n}[\ddot{\phi}_i \sin(\phi_i + \omega t - \theta) \\ & + (\dot{\phi}_i + \omega)^2 \cos(\phi_i + \omega t - \theta)] = M\varepsilon\omega^2 \cos(\omega t - \theta), \end{aligned} \tag{8}$$

$$\begin{aligned} & (M + nm)(r\ddot{\theta} - 2\dot{r}\dot{\theta}) + cr\dot{\theta} + mR\sum_{i=1}^{n}[\ddot{\phi}_i \cos(\phi_i + \omega t - \theta) \\ & - (\dot{\phi}_i + \omega)^2 \sin(\phi_i + \omega t - \theta)] = M\varepsilon\omega^2 \sin(\omega t - \theta), \end{aligned} \tag{9}$$

$$\begin{aligned} & mR^2\ddot{\phi}_i + D\dot{\phi}_i - mR(\ddot{r} - r\dot{\theta}^2)\sin(\phi_i + \omega t - \theta) + mR(r\ddot{\theta} + 2\dot{r}\dot{\theta})\cos(\phi_i + \omega t - \theta) \\ & = 0, \quad i = 1, 2, \ldots, n. \end{aligned} \tag{10}$$

During the derivation, the angular speed ω is assumed constant. In the case that there is no ball, i.e., $m = 0$, the equations of motion (8)–(10) reduce to th equations for the Jeffcott rotor which are expressed as

$$M(\ddot{r} - r\dot{\theta}^2) + c\dot{r} + kr = M\varepsilon\omega^2 \cos(\omega t - \theta), \tag{11}$$

$$M(r\ddot{\theta} + 2\dot{r}\dot{\theta}) + cr\,\dot{\theta} = M\varepsilon\omega^2 \sin(\omega t - \theta). \tag{12}$$

3. EQUILIBRIUM POSITIONS AND LINEAR VARIATIONAL EQUATIONS

Stability analysis can be carried out easily by transforming the equations of motion for a non-autonomous system into those for an autonomous system. As seen in equations (8)–(10), the equations of motion correspond to the non-autonomous system. Generally, it is very cumbersome to analyze the stability for non-autonomous systems. If the stability analysis is performed for the non-autonomous system, the linearized equations of motion around equilibrium positions become ordinary differential equations with parametric excitation. In this case, the stability analysis requires the application of the Floquet theory, which results in inaccuracy and much computation time. On the other hand, since θ increases monotonically with time, it is impossible to determine the equilibrium positions with respect to θ. To overcome the above difficulties, this study uses a generalized co-ordinate ψ instead of θ, which is defined by

$$\psi = \omega t - \theta. \tag{13}$$

The generalized co-ordinate ψ represents the angle from the r direction to the centre of mass G, as shown in Figure 2.

Since the state equations can be conveniently used to analyze the stability of the system, using equation (13), let us rewrite the equations of motion (8)–(10) as the state equations. To do this, it is necessary to denote the velocities, $\dot{r}$, $\dot{\psi}$, and $\dot{\phi}_i$ by new symbols:

$$\dot{r} \overset{\text{def}}{=} \hat{r}, \quad \dot{\psi} \overset{\text{def}}{=} \hat{\psi}, \quad \dot{\phi}_i \overset{\text{def}}{=} \hat{\phi}_i. \tag{14}$$

Substituting equation (13) into equations (8)–(10) and using the notations given by equation (14), the equations of motion can be expressed as the state equations which are $2n + 4$ first-order differential equations. The state equations may be written by a matrix–vector equation

$$\mathbf{A}(\mathbf{x})\dot{\mathbf{x}} = \mathbf{N}(\mathbf{x}), \tag{15}$$

and

$$\mathbf{x} = \{r, \psi, \phi_1, \phi_2, \ldots, \phi_n, \hat{r}, \hat{\psi}, \hat{\phi}_1, \hat{\phi}_2, \ldots, \hat{\phi}_n]^T, \tag{16}$$

$$\mathbf{A} = \begin{bmatrix} \mathbf{I} & \mathbf{0} \\ \mathbf{0} & \mathbf{M} \end{bmatrix}, \tag{17}$$

$$\mathbf{N} = \{N_r, N_\psi, N_{\phi 1}, N_{\phi 2}, \ldots, N_{\phi n}, N_{\hat{r}}, N_{\hat{\psi}}, N_{\hat{\phi}^1}, N_{\hat{\phi}^2}, \ldots, N_{\hat{\phi}n}\}^T, \tag{18}$$

in which $\mathbf{I}$ is the $(n+2)\times(n+2)$ identity matrix and

$$\mathbf{M} = \begin{bmatrix} M+nm & 0 & -mRS_1 & -mRS_2 & \cdots & -mRS_n \\ 0 & (M+nm)r & -mRC_1 & -mRC_2 & \cdots & -mRC_n \\ -mRS_1 & -mRrC_1 & mR^2 & 0 & \cdots & 0 \\ -mRS_2 & -mRrC_2 & 0 & mR^2 & \cdots & 0 \\ \vdots & \vdots & \vdots & \vdots & \ddots & \vdots \\ -mRS_n & -mRrC_n & 0 & 0 & \cdots & mR^2 \end{bmatrix}, \tag{19}$$

$$N_r = \hat{r}, \tag{20}$$

$$N_\psi = \hat{\psi}, \tag{21}$$

$$N_{\phi i} = \hat{\phi}_i, \quad i = 1,2,\ldots,n, \tag{22}$$

$$N_{\hat{r}} = (M+nm)\,r\,(\omega-\hat{\psi})^2 - c\hat{r} - kr + M\varepsilon\omega^2\cos\psi + mR\sum_{i=1}^{n}(\hat{\phi}_i+\omega)^2\cos(\phi_i+\psi), \tag{23}$$

$$N_{\hat{\psi}} = 2(M+nm)\,\hat{r}(\omega-\hat{\psi}) + cr(\omega-\hat{\psi}) - M\varepsilon\omega^2\sin\psi - mR\sum_{i=1}^{n}(\hat{\phi}_i+\omega)^2\sin(\phi_i+\psi), \tag{24}$$

$$N_{\hat{\phi}i} = -D\hat{\phi}_i - mRr(\omega-\hat{\psi})^2\sin(\phi_i+\psi) - 2mR\hat{r}(\omega-\hat{\psi})\cos(\phi_i+\psi), \quad i = 1,2,\ldots,n. \tag{25}$$

In equation (19), S_i and C_i are given by

$$S_i = \sin(\phi_i+\psi), \quad C_i = \cos(\phi_i+\psi). \tag{26}$$

Notice that equation (15) is for an autonomous system so the stability is easily analyzed.

The equilibrium positions are obtained from equation (15) by letting $\dot{\mathbf{x}} = \mathbf{0}$. That is, they are computed from

$$\mathbf{N}(\mathbf{x}^*) = 0, \tag{27}$$

where $\mathbf{x}^*$ represents the equilibrium positions denoted by

$$\mathbf{x}^* = \{r^*, \psi^*, \phi_1^*, \phi_2^*, \ldots, \phi_n^*, \hat{r}^*, \hat{\psi}^*, \hat{\phi}_1^*, \hat{\phi}_2^*, \ldots, \hat{\phi}_n^*\}^{\mathrm{T}}. \tag{28}$$

In other words, the constant $r^*, \psi^*, \phi_i^*, \hat{r}^*, \hat{\psi}^*$ and $\hat{\phi}_i^*$ are determined by solving the $2n+4$ algebraic equations represented by equation (27). The algebraic equations are simplified as

$$\hat{r}^* = 0, \quad \hat{\psi}^* = 0, \quad \hat{\phi}_i^* = 0, \quad i = 1,2,\ldots,n, \tag{29}$$

$$[k-(M+nm)\,\omega^2]\,r^* - mR\omega^2\sum_{i=1}^{n}\cos(\phi_i^*+\psi^*) = M\varepsilon\omega^2\cos\psi^*, \tag{30}$$

$$c\omega r^* - mR\omega^2 \sum_{i=1}^{n} \sin(\phi_i^* + \psi^*) = M\varepsilon\omega^2 \sin\psi^*, \tag{31}$$

$$r^* \sin(\phi_i^* + \psi^*) = 0, \quad i = 1,2, \ldots, n. \tag{32}$$

The equilibrium positions may be classified into two cases: the balanced and unbalanced cases, which correspond to $r^* = 0$ and $r^* \neq 0$ respectively. When the system is balanced, i.e., $r^* = 0$, equations (30) and (31) can be rewritten as

$$\frac{\varepsilon}{R} + \frac{m}{M} \sum_{i=1}^{n} \cos\phi_i^* = 0, \tag{33}$$

$$\sum_{i=1}^{n} \sin\phi_i^* = 0. \tag{34}$$

Equations (33) and (34) imply that the balls balance the disk statically with positions given by ϕ_i^*. On the other hand, when the system has the unbalanced equilibrium positions ($r^* \neq 0$), the values of r^*, ψ^* and ϕ_i^* can be determined from equations (30)–(32):

$$r^* = \frac{\alpha mR\omega^2 [k - (M + nm)\omega^2] \pm M\varepsilon\omega^2 \sqrt{[k - (M + nm)\omega^2]^2 + [1 - (\alpha mR/M\varepsilon)^2]\, c^2\, \omega^2}}{[k - (M + nm)\omega^2]^2 + c^2\omega^2}, \tag{35}$$

$$\psi^* = \tan^{-1} \frac{c\omega r^*}{[k - (M + nm)\omega^2]\ r^* - \alpha mR\omega^2}, \tag{36}$$

$$\phi_i^* = \alpha_i \pi - \psi^*, \quad i = 1, 2, \ldots, n, \tag{37}$$

where α_i are integers depending on the positions of the balls and

$$\alpha = \sum_{i=1}^{n} (-1)^{\alpha_i}. \tag{38}$$

It is noted that the value of r^* in equation (35) should be real and positive. If r^* is negative or complex, this means that the equilibrium positions defined by equations (35)–(37) do not exist. In the case that the system has no ball, equations (35) and (36) are reduced to

$$r^* = \frac{M\varepsilon\omega^2}{\sqrt{(k - M\omega^2)^2 + c^2\omega^2}}, \tag{39}$$

$$\psi^* = \tan^{-1} \frac{c\omega}{k - M\omega^2}, \tag{40}$$

which are the amplitude and phase of the Jeffcott rotor respectively.

The perturbation method is used to derive linear variational equations from the non-linear equations of motion. The perturbed motion in the neighborhood of the equilibrium positions can be expressed in the form

$$\mathbf{x} = \mathbf{x}^* + \Delta\mathbf{x}, \tag{41}$$

where $\Delta\mathbf{x}$ is the perturbation of $\mathbf{x}$:

$$\Delta\mathbf{x} = \{\Delta r, \Delta\psi, \Delta\phi_1, \Delta\phi_2, \ldots, \Delta\phi_n, \Delta\hat{r}, \Delta\hat{\psi}, \Delta\hat{\phi}_1, \Delta\hat{\phi}_2, \ldots, \Delta\hat{\phi}_n\}^{\mathrm{T}}, \tag{42}$$

in which Δr, $\Delta\psi$, $\Delta\phi_i$, $\Delta\hat{r}$, $\Delta\hat{\psi}$ and $\Delta\hat{\phi}_i$ are small variations of r, ψ, ϕ_i, $\hat{r}$, $\hat{\psi}$ and $\hat{\phi}_i$ respectively. Introducing equation (41) into equation (15) and recalling that $\mathbf{x}^*$ satisfies equation (27), equation (15) can be written as

$$\mathbf{A}(\mathbf{x}^* + \Delta\mathbf{x})\,\Delta\dot{\mathbf{x}} = \mathbf{N}(\mathbf{x}^* + \Delta\mathbf{x}) - \mathbf{N}(\mathbf{x}^*). \tag{43}$$

Since $\Delta\mathbf{x} = \mathbf{0}$ is a trivial solution of equation (43), expanding equation (43) about $\Delta\mathbf{x} = \mathbf{0}$ results in

$$\mathbf{A}^*\,\Delta\dot{\mathbf{x}} = \mathbf{B}^*\Delta\mathbf{x} + \mathbf{O}(\Delta\mathbf{x}), \tag{44}$$

where $\mathbf{A}^*$ and $\mathbf{B}^*$ are constant and $\mathbf{O}$ is a function of $\Delta\mathbf{x}$ with a second and higher order. The $\mathbf{A}^*$ and $\mathbf{B}^*$ matrices are defined by

$$\mathbf{A}^* = \mathbf{A}(\mathbf{x}^*), \tag{45}$$

$$\mathbf{B}^* = \begin{bmatrix} \mathbf{0} & \mathbf{I} \\ -\mathbf{K}^* & -\mathbf{C}^* \end{bmatrix}, \tag{46}$$

where

$$\mathbf{C}^* = \begin{bmatrix} c & 2(M+nm)\omega r^* & -2mR\omega C_1^* & -2mR\omega C_2^* & \cdots & -2mR\omega C_n^* \\ -2(M+nm)\,\omega & cr^* & 2mR\omega S_1^* & 2mR\omega S_2^* & \cdots & 2mR\omega S_n^* \\ 2mR\omega C_1^* & 0 & D & 0 & \cdots & 0 \\ 2mR\omega C_2^* & 0 & 0 & D & \cdots & 0 \\ \vdots & \vdots & \vdots & \vdots & \ddots & \vdots \\ 2mR\omega C_n^* & 0 & 0 & 0 & \cdots & D \end{bmatrix}, \tag{47}$$

$$\mathbf{K}^* =$$

$$\begin{bmatrix}
k-(M+nm)\omega^2 & \omega^2\left(M\varepsilon\sin\psi^* + mR\sum_{i=1}^{n} S_i^*\right) & mR\omega^2 S_1^* & mR\omega^2 S_2^* & \cdots & mR\omega^2 S_n^* \\
-c\omega & \omega^2\left(M\varepsilon\cos\psi^* + mR\sum_{i=1}^{n} C_i^*\right) & mR\omega^2 C_1^* & mR\omega^2 C_2^* & \cdots & mR\omega^2 C_n^* \\
mR\omega^2 S_1^* & mR\omega^2 r^* C_1^* & mR\omega^2 r^* C_1^* & 0 & \cdots & 0 \\
mR\omega^2 S_2^* & mR\omega^2 r^* C_2^* & 0 & mR\omega^2 r^* C_2^* & \cdots & 0 \\
\vdots & \vdots & \vdots & \vdots & \ddots & \vdots \\
mR\omega^2 S_n^* & mR\omega^2 r^* C_n^* & 0 & 0 & \cdots & mR\omega^2 r^* C_n^*
\end{bmatrix} \tag{48}$$

in which

$$S_i^* = \sin(\phi_i^* + \psi^*), \quad C_i^* = \cos(\phi_i^* + \psi^*). \tag{49}$$

Equations (47) and (48) may be simplified by using the equations for the equilibrium positions given by equations (30)–(32). Assuming that the perturbation $\Delta\mathbf{x}$ is sufficiently small to permit $\mathbf{O}$ to be ignored, equation (44) can be approximated by

$$\mathbf{A}^*\Delta\dot{\mathbf{x}} = \mathbf{B}^*\Delta\mathbf{x}, \tag{50}$$

which represents the linear variational equation. Note that equation (50) is confined to the neighborhood of the equilibrium positions.

4. STABILITY ANALYSIS

The stability of the system in the neighborhood of the equilibrium positions is analyzed with the linear variational equations given by equation (50). For simplicity of the analysis, consider the case that the ADB has two balls, i.e., $n = 2$. Then the $\mathbf{A}^*$ and $\mathbf{B}^*$ matrices become 8×8 matrices. The stability around the equilibrium positions can be investigated with the eigenvalue problem for equation (50). Let a solution of equation (50) be

$$\Delta\mathbf{x} = \Delta\mathbf{X}e^{\lambda t}, \tag{51}$$

where λ is an eigenvalue and $\Delta\mathbf{X}$ is an eigenvector corresponding to λ. The eigenvector can be denoted by

$$\Delta\mathbf{X} = \{\Delta R, \Delta\Psi, \Delta\Theta_1, \Delta\Theta_2, \Delta\hat{R}, \Delta\hat{\Psi}, \Delta\hat{\Theta}_1, \Delta\hat{\Theta}_2\}^{\mathrm{T}}. \tag{52}$$

Introducing equation (51) in equation (50) yields the eigenvalue problem defined by

$$(\mathbf{B}^* - \lambda\mathbf{A}^*)\,\Delta\mathbf{X} = 0. \tag{53}$$

As is well known, the system is asymptotically stable, when all the eigenvalues have negative real parts. On the contrary, if at least one of the eigenvalues has a positive real part, the system is unstable. The eigenvalues can be computed by solving the characteristic equation obtained by setting

$$\det(\mathbf{B}^* - \lambda \mathbf{A}^*) = 0, \tag{54}$$

which can be expressed as a polynomial of λ:

$$c_0\left(\frac{\lambda}{\omega_n}\right)^8 + c_1\left(\frac{\lambda}{\omega_n}\right)^7 + c_2\left(\frac{\lambda}{\omega_n}\right)^6 + c_3\left(\frac{\lambda}{\omega_n}\right)^5 + c_4\left(\frac{\lambda}{\omega_n}\right)^4 + c_5\left(\frac{\lambda}{\omega_n}\right)^3 + c_6\left(\frac{\lambda}{\omega_n}\right)^2 + c_7\frac{\lambda}{\omega_n} + c_8 = 0, \tag{55}$$

where ω_n is the natural frequency of the system without balls, defined by $\omega_n = \sqrt{k/M}$.

First, consider the characteristic equation for the stability in the neighborhood of the equilibrium positions corresponding to $r^* = 0$. When the ADB has only two balls, the equilibrium positions for the balls are determined from equations (33) and (34):

$$\phi_1^* = -\phi_2^* = \tan^{-1}\frac{\sqrt{(2(m/m)/(\varepsilon/R))^2 - 1}}{-1}. \tag{56}$$

As seen in equation (56), in order that ϕ_1^* and ϕ_2^* exist when $r^* = 0$, the ball mass satisfies the condition given by

$$\frac{m}{M} \geqslant \frac{1}{2}\frac{\varepsilon}{R}. \tag{57}$$

Since the equilibrium position of ψ^* is not defined when $r^* = 0$, the characteristic equation cannot be determined directly from equation (54). This means that a special treatment is required to obtain the characteristic equation. Equation (53) represents eight linear algebraic equations with nine unknows (ΔR, $\Delta\Psi$, $\Delta\Theta_1$, $\Delta\Theta_2$, $\Delta\hat{R}$, $\Delta\hat{\Psi}$, $\Delta\hat{\Theta}_1$, $\Delta\hat{\Theta}_2$ and ψ^*); therefore, an additional equation is required for equation (53) to have a non-trivial solution. This equation is given by the identity equation

$$\sin^2\psi^* + \cos^2\psi^* = 1. \tag{58}$$

Eliminating ψ^* by some algebraic manipulations for equations (53) and (58), we obtain the characteristic equation in the form of equation (55). The coefficients of equation (55) are as follows:

$$c_0 = -(\bar{\varepsilon}^2 + 2\bar{m})(\bar{\varepsilon}^2 - 2\bar{m} - 4\bar{m}^2), \tag{59}$$

$$c_1 = 8\bar{m}^2(1 + \bar{m})(\bar{\beta} + 2\bar{m}\bar{\beta} + 2\zeta), \tag{60}$$

$$c_2 = 4\bar{m}^2(2 + 2\bar{m} + \bar{\beta}^2 + 4\bar{m}\bar{\beta}^2 + 4\bar{m}^2\bar{\beta}^2 + 8\bar{\beta}\zeta + 12\bar{m}\bar{\beta}\zeta + 4\zeta^2) - 4(\bar{\varepsilon}^4 - 2\bar{m}^2 - 4\bar{\varepsilon}^2\bar{m}^2 - 6\bar{m}^3 - 4\bar{m}^4)\,\bar{\omega}^2, \tag{61}$$

$$c_3 = 8\bar{m}^2\,[(2\bar{\beta} + 3\bar{m}\bar{\beta} + 2\zeta + 2\bar{\beta}^2\zeta + 4\bar{m}\bar{\beta}^2\zeta + 4\bar{\beta}\zeta^2) + (2\bar{\beta} + 7\bar{m}\bar{\beta} + 6\bar{m}^2\,\bar{\beta} + 2\zeta + 8\bar{m}\zeta)\,\bar{\omega}^2], \tag{62}$$

$$c_4 = 4\bar{m}^2(1 + 2\bar{\beta}^2 + 4\bar{m}\bar{\beta}^2 + 8\bar{\beta}\zeta + 4\bar{\beta}^2\zeta^2) + 8\bar{m}^2(-1 + 4\bar{m} + \bar{\beta}^2 + 4\bar{m}\bar{\beta}^2 + 4\bar{m}^2\,\bar{\beta}^2 + 4\bar{\beta}\zeta + 12\bar{m}\bar{\beta}\zeta + 2\zeta^2)\bar{\omega}^2 + (-6\bar{\varepsilon}^4 + 4\bar{m}^2 + 24\bar{\varepsilon}^2\bar{m}^2 + 24\bar{m}^3 + 32\bar{m}^4)\,\bar{\omega}^4, \tag{63}$$

$$c_5 = 8\bar{m}^2\,[\bar{\beta}(1 + 2\bar{\beta}\zeta) + 2\bar{\beta}(-1 + \bar{m} + \bar{\beta}\zeta + 2\bar{m}\bar{\beta}\zeta + 2\zeta^2)\,\bar{\omega}^2 + (\bar{\beta} + 5\bar{m}\,\bar{\beta} + 6\bar{m}^2\,\bar{\beta} + 6\bar{m}\,\zeta)\,\bar{\omega}^4], \tag{64}$$

$$c_6 = 4\bar{m}^2\,\bar{\beta}^2 - 8\bar{m}^2\,\bar{\beta}^2(1 + 2\bar{m} - 2\zeta^2)\,\bar{\omega}^2 + 4\bar{m}^2(-2\bar{m} + \bar{\beta}^2 + 4\bar{m}\bar{\beta}^2 + 4\bar{m}^2\bar{\beta}^2 + 12\bar{m}\bar{\beta}\zeta)\,\bar{\omega}^4 - 4(\bar{\varepsilon}^4 - 4\bar{\varepsilon}^2\,\bar{m}^2 - 2\bar{m}^3 - 4\bar{m}^4)\,\bar{\omega}^6, \tag{65}$$

$$c_7 = 8\bar{m}^3\,\bar{\beta}\,(-1 + \bar{\omega}^2 + 2\bar{m}\bar{\omega}^2)\,\bar{\omega}^4, \tag{66}$$

$$c_8 = -\,\bar{\varepsilon}^2\,(\bar{\varepsilon} - 2\bar{m})(\bar{\varepsilon} + 2\bar{m})\,\bar{\omega}^8, \tag{67}$$

where ζ is the damping factor of the system given by

$$\zeta = \frac{c}{2\sqrt{Mk}}, \tag{68}$$

and $\bar{m}$, $\bar{\varepsilon}$, $\bar{\omega}$ and $\bar{\beta}$ are non-dimensional parameters defined by

$$\bar{m} = \frac{m}{M}, \quad \bar{\varepsilon} = \frac{\varepsilon}{R}, \quad \bar{\omega} = \frac{\omega}{\omega_n}, \quad \bar{\beta} = \frac{D}{mR^2\,\omega_n^2}. \tag{69}$$

Next, consider the equilibrium positions and characteristic equation when $r^* \neq 0$. In this case, the equilibrium positions are computed from equations (35) to (37). The equilibrium positions possessing the stable region are expressed by

$$\frac{r^*}{R} = \frac{2\bar{m}\bar{\omega}^2\,[1 - (1 + 2\bar{m})\,\bar{\omega}^2] + \bar{\varepsilon}\bar{\omega}^2\,\sqrt{[1 - (1 + 2\bar{m})\,\bar{\omega}^2]^2 + [1 - (2\bar{m}/\bar{\varepsilon})^2]\;(2\zeta\bar{\omega})^2}}{[1 - (1 + 2\bar{m})\,\bar{\omega}^2]^2 + (2\zeta\bar{\omega})^2}, \tag{70}$$

$$\psi^* = \tan^{-1}\frac{2\zeta\bar{\omega}r^*}{[1 - (1 + 2\bar{m})\,\bar{\omega}^2]\;r^* - 2R\bar{m}\bar{\omega}^2}, \tag{71}$$

$$\phi_1^* = \phi_2^* = -\,\psi^*. \tag{72}$$

In fact, there exists other equilibrium positions different from the positions defined by equations (70)–(72). However, since these positions are unstable singular points under any circumstance, we do not have further discussion about them. Substituting r^*, ψ^*, ϕ_1^* and ϕ_2^* given by equations (70)–(72) into equation (54), we can easily obtain the characteristic polynomial in the form of equation (55). The coefficients of the polynomial are too complicated to express them in closed forms, so they are not presented in this paper.

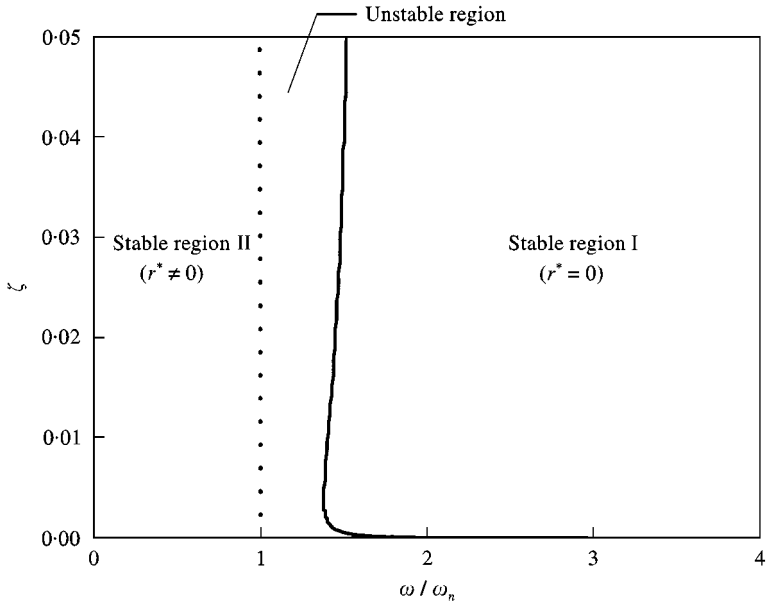

Figure 3. Stability for the variation of ω/ω_n and ζ when $m/M = \varepsilon/R = \bar{\beta} = 0{\cdot}01$.

The Routh–Hurwitz criteria are used to investigate the stability of the system, because it may be a formidable task to solve the characteristic equation accurately. The Routh–Hurwitz criteria provide the necessary and sufficient conditions for all the roots of the characteristic equation to have negative real parts. The stability of the system is investigated for the variations of the non-dimensional system parameters such as ω/ω_n, m/M, ε/R, ζ and $\bar{\beta}$. Considering the variations of all the system parameters hinders the efficient description of the stability; hence, the stability is checked with the variations for a pair of parameters, for example, ω/ω_n versus ζ, ω/ω_n versus $\bar{\beta}$, ω/ω_n versus ε/R, ω/ω_n versus m/M, or ε/R versus m/M.

The influence of the energy dissipation factors, ζ and $\bar{\beta}$, on the stability of the system is analyzed in the neighborhood of the equilibrium positions. When $m/M = \varepsilon/R = \bar{\beta} = 0{\cdot}01$, the stability for the variations of ω/ω_n and ζ is presented in Figure 3. The stable region I bounded by the solid line represents the stable region for the equilibrium positions corresponding to $r^* = 0$ while the stable region II bounded by the dotted line represents the stable region for the equilibrium positions corresponding to $r^* \neq 0$. If the values of ω/ω_n and ζ are inside the stable region I, the ADB is working, that is, the rotor system becomes balanced. Otherwise, the system is not balanced even though the values of ω/ω_n and ζ are in the stable region II. The effect of $\bar{\beta}$ on the stability is similar to that of ζ, as shown in Figure 4. So the ADB cannot perform its function for the conservative system in which $\zeta = \bar{\beta} = 0$. Consequently, the energy dissipation characteristics are essential for the ADB to obtain balancing. It is interesting that in some experiments the system with $\zeta \neq 0$ becomes balanced even when it has no damping fluid, i.e., $\bar{\beta} = 0$. It is believed that this phenomenon occurs due to the friction between the race and balls, because the friction is also a dissipation mechanism of energy.

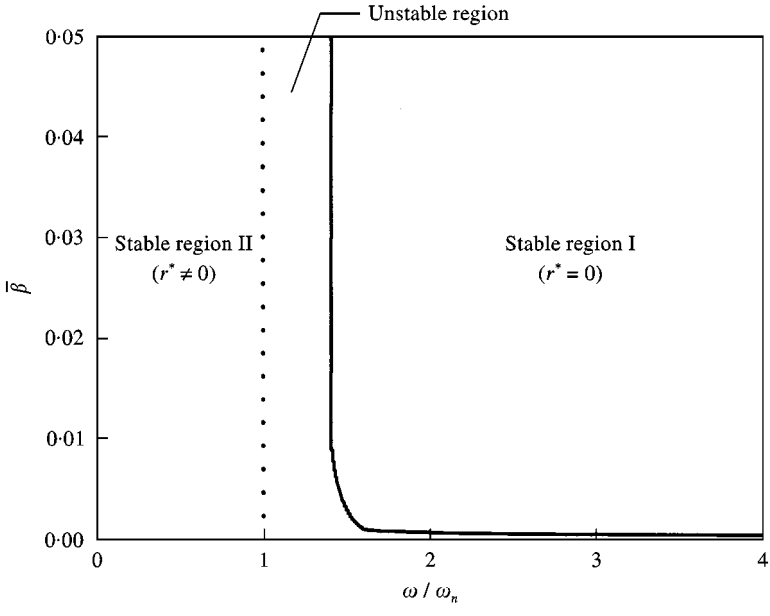

Figure 4. Stability for the variation of ω/ω_n and $\bar{\beta}$ when $m/M = \varepsilon/R = \zeta = 0{\cdot}01$.

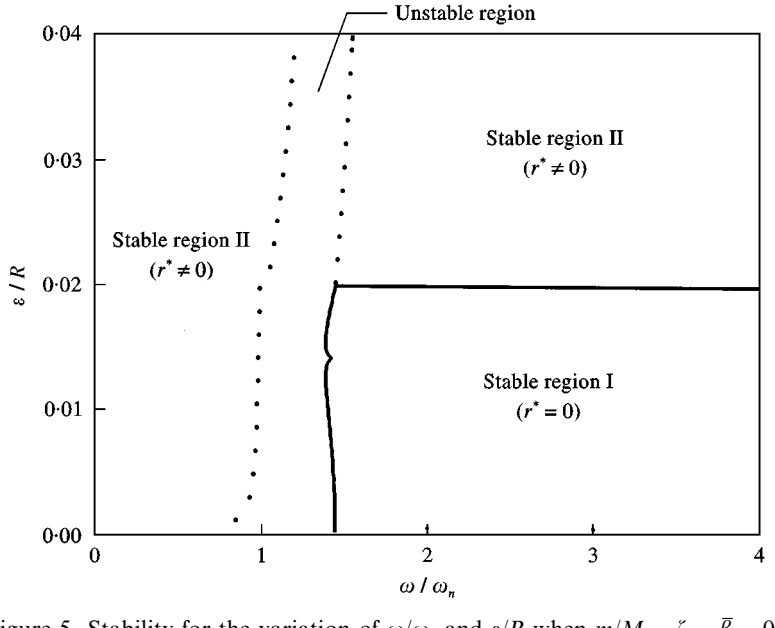

Figure 5. Stability for the variation of ω/ω_n and ε/R when $m/M = \zeta = \bar{\beta} = 0{\cdot}01$.

Notice that the system is in the stable region II regardless of the values of ζ and $\bar{\beta}$, when the operating speed is below the critical speed, i.e., $\omega/\ \omega_n < 1$.

The eccentricity of the rotor and the mass of the ball also have an influence on the stability of the system. The balancing of the system can be obtained only if the eccentricity and ball mass satisfy the condition given by equation (57). The boundary of this condition is represented by the straight solid lines in Figures 5

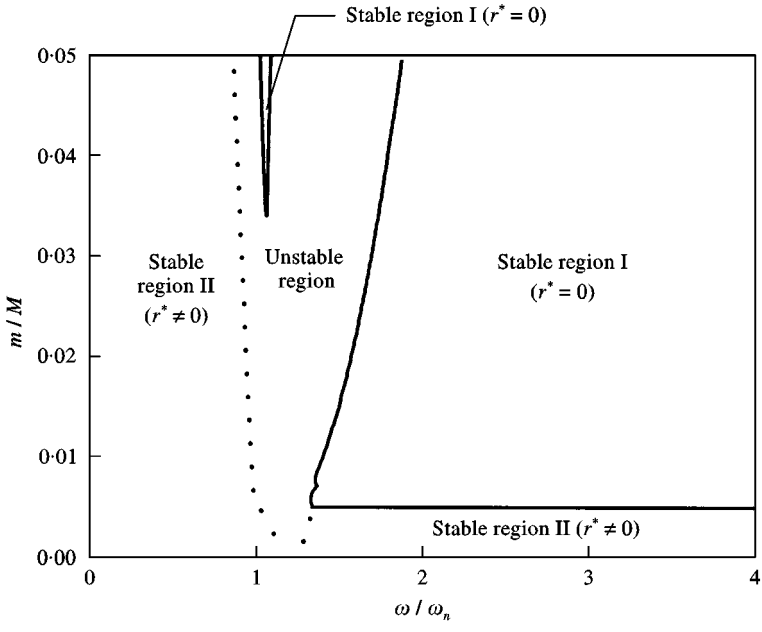

Figure 6. Stability for the variation of ω/ω_n and m/M when $\varepsilon/R = \zeta = \bar{\beta} = 0{\cdot}01$.

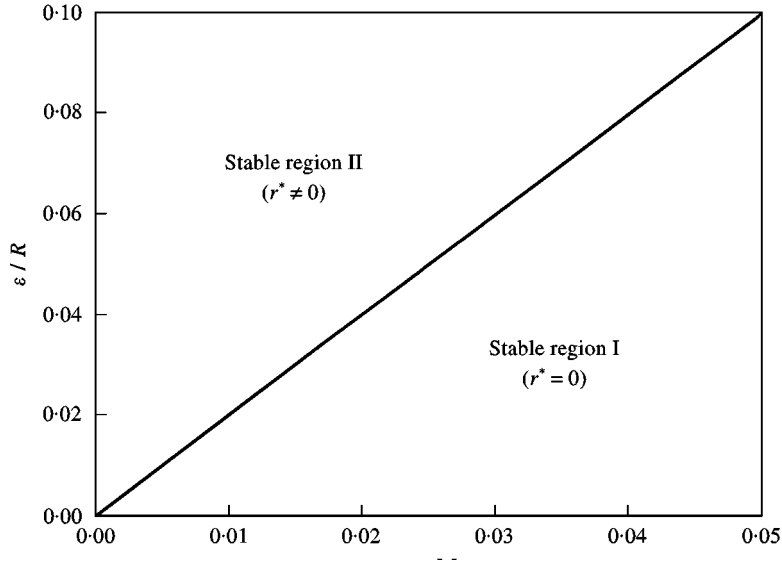

Figure 7. Stability for the variation of m/M when ε/R when $\omega/\omega_n = 2$ and $\zeta = \bar{\beta} = 0{\cdot}01$.

and 6. Figure 5 describes the stability for ω/ω_n versus ε/R with the fixed values of $m/M = \zeta = \bar{\beta} = 0{\cdot}01$, while Figure 6 describes the stability for ω/ω_n versus m/M with $\varepsilon/R = \zeta = \bar{\beta} = 0{\cdot}01$. Figures 5 and 6 show that the system is stable around the equilibrium position corresponding to $r^* \neq 0$ if the operating speed ω is approximately less than the critical speed ω_n. When ω/ω_n, ε/R and m/M are in the unstable regions of Figures 5 and 6, the system is unstable in the neighborhood of the equilibrium positions corresponding to both $r^* = 0$ and $r^* \neq 0$. Therefore, the

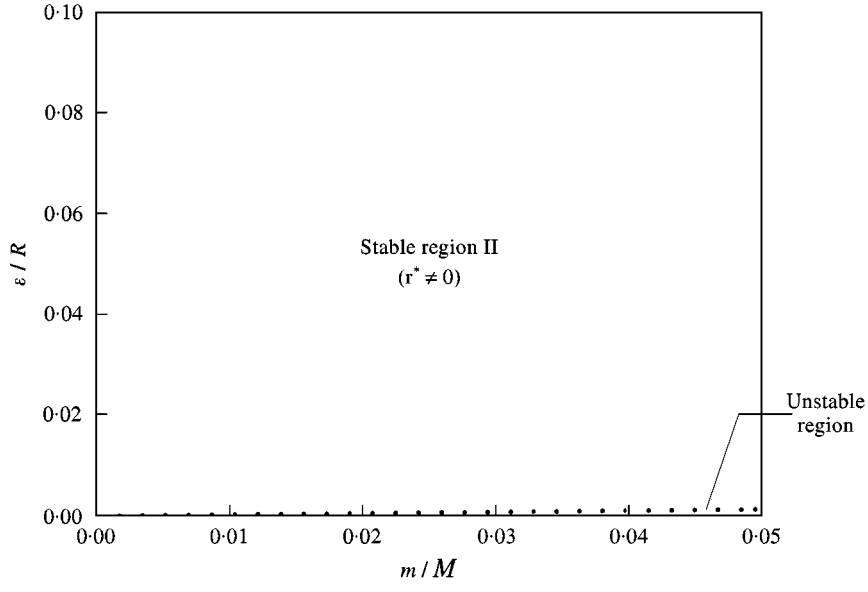

Figure 8. Stability for the variation of m/M and ε/R when $\omega/\omega_n = 0{\cdot}5$ and $\zeta = \bar{\beta} = 0{\cdot}01$.

ADB should not only be designed to satisfy that m/M is greater than $\varepsilon/2R$, but ω/ω_n, ε/R and m/M should also be carefully chosen to guarantee stability. As shown in Figure 6, the lower limit of ω/ω_n, in the stable region I decreases as m/M increases with the fixed value of the eccentricity. In the cases of $\omega/\omega_n = 2$ and $\omega/\omega_n = 0{\cdot}5$ with $\zeta = \bar{\beta} = 0{\cdot}01$, the stability for the variations of ε/R and m/M is plotted in Figures 7 and 8 respectively. When $\omega/\ \omega_n = 2$, the stable regions I and II are divided by the line $\varepsilon/R = nm/M$, as shown in Figure 7. However, when $\omega/\omega_n = 0{\cdot}5$, as shown in Figure 8, the stable region I does not exist and the system is in the stable region II with the exception of the region for small ε/R.

5. TIME RESPONSES

To verify the stability analyzed in the previous section and to analyze the dynamic behavior of the system, the time responses of the non-linear equations are computed by a direct time integration method. For computation of the responses, this study adopts the generalized-α method that is an implicit time integration method. Since the generalized-α method is unconditionally stable, it has an advantage to choose larger time steps than an explicit method. For example, if the Runge–Kutta method is applied to this problem, very small time steps are required to obtain the time responses. To apply the generalized-α method to the non-linear equations, it is convenient to express equation (15) as a second order non-linear differential equation

$$\mathbf{G}(\mathbf{y}, \dot{\mathbf{y}}, \ddot{\mathbf{y}}) = \mathbf{M}(\mathbf{y})\ddot{\mathbf{y}} + \mathbf{F}(\mathbf{y}, \dot{\mathbf{y}}) = \mathbf{0}, \tag{73}$$

where

$$\mathbf{y} = \{r, \psi, \phi_1, \phi_2\}^T \tag{74}$$

$$\mathbf{M} =$$

$$\begin{bmatrix} M+2m & 0 & -mR\sin(\phi_1+\psi) & -mR\sin(\phi_2+\psi) \\ 0 & (M+2m)r & -mR\cos(\phi_1+\psi) & -mR\cos(\phi_2+\psi) \\ -mR\sin(\phi_1+\psi) & -mRr\cos(\phi_1+\psi) & mR^2 & 0 \\ -mR\sin(\phi_2+\psi) & -mRr\cos(\phi_2+\psi) & 0 & mR^2 \end{bmatrix} \tag{75}$$

$$\mathbf{F} =$$

$$\begin{Bmatrix} -(M+2m)r(\omega-\dot{\psi})^2 + c\dot{r} + kr - M\varepsilon\omega^2\cos\psi - mR\sum_{i=1}^{2}(\dot{\phi}_i+\omega)^2\cos(\phi_i+\psi) \\ -2(M+2m)\dot{r}(\omega-\dot{\psi}) - cr(\omega-\dot{\psi}) + M\varepsilon\omega^2\sin\psi + mR\sum_{i=1}^{2}(\dot{\phi}_i+\omega)^2\sin(\phi_i+\psi) \\ D\dot{\phi}_1 + mRr(\omega-\dot{\psi})^2\sin(\phi_1+\psi) + 2mR\dot{r}(\omega-\dot{\psi})\cos(\phi_1+\psi) \\ D\dot{\phi}_2 + mRr(\omega-\dot{\psi})^2\sin(\phi_2+\psi) + 2mR\dot{r}(\omega-\dot{\psi})\cos(\phi_2+\psi) \end{Bmatrix}. \tag{76}$$

The generalized-α method for equation (73) is given by

$$\mathbf{M}(\mathbf{d}_{n+1-\alpha_f})\,\mathbf{a}_{n+1-\alpha_m} + \mathbf{F}(\mathbf{d}_{n+1-\alpha_f},\ \mathbf{v}_{n+1-\alpha_f}) = \mathbf{0}, \tag{77}$$

$$\mathbf{d}_{n+1} = \tilde{\mathbf{d}}_n + \beta\Delta t^2\,\mathbf{a}_{n+1}, \tag{78}$$

$$\mathbf{v}_{n+1} = \tilde{\mathbf{v}}_n + \gamma\Delta t\mathbf{a}_{n+1}, \tag{79}$$

where

$$\tilde{\mathbf{d}}_n = \mathbf{d}_n + \Delta t\mathbf{v}_n + (1/2-\beta)\,\Delta t^2\,\mathbf{a}_n, \tag{80}$$

$$\tilde{\mathbf{v}}_n = \mathbf{v}_n + (1-\gamma)\,\Delta t\mathbf{a}_n, \tag{81}$$

$$\mathbf{d}_{n+1-\alpha_f} = (1-\alpha_f)\,\mathbf{d}_{n+1} + \alpha_f\,\mathbf{d}_n, \tag{82}$$

$$\mathbf{v}_{n+1-\alpha_f} = (1-\alpha_f)\,\mathbf{v}_{n+1} + \alpha_f\,\mathbf{v}_n, \tag{83}$$

$$\mathbf{a}_{n+1-\alpha_m} = (1-\alpha_m)\,\mathbf{a}_{n+1} + \alpha_m\,\mathbf{a}_n, \tag{84}$$

in which $\mathbf{d}_n$, $\mathbf{v}_n$ and $\mathbf{a}_n$ are approximations to $\mathbf{y}(t_n)$, $\dot{\mathbf{y}}(t_n)$ and $\ddot{\mathbf{y}}(t_n)$ respectively; $\Delta t = t_{n+1} - t_n$ is the time step; α_f, α_m, β, γ are the algorithmic parameters of the generalized α method. When the parameter for the numerical dissipation ρ_∞ is specified, the above algorithmic parameters are determined. See reference [4] for the details of the generalized-α method. The initial conditions for the time integration are given by

$$\mathbf{d}_0 = \mathbf{y}(0), \tag{85}$$

$$\mathbf{v}_0 = \dot{\mathbf{y}}(0), \tag{86}$$

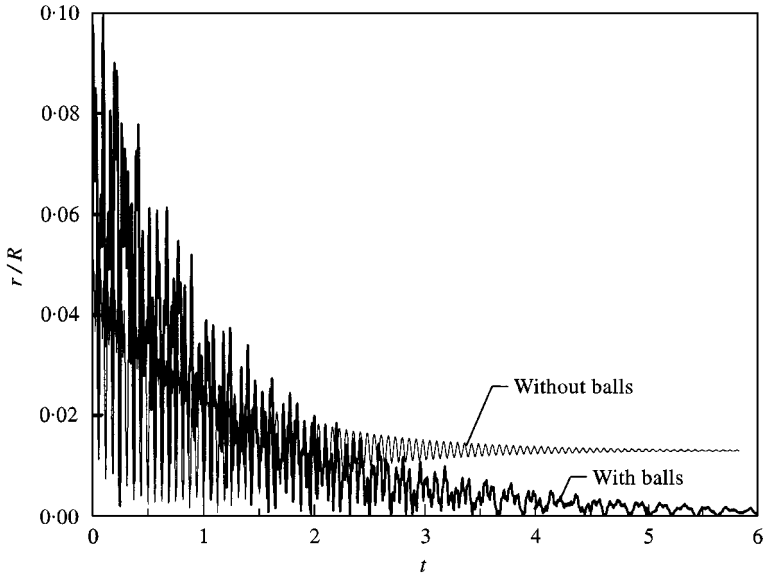

Figure 9. Time response of the radial displacement when $\omega/\omega_n = 2$ and $m/M = \varepsilon/R = \zeta = \bar{\beta} = 0{\cdot}01$.

$$\mathbf{a}_0 = -\mathbf{M}^{-1}(y(0))\,\mathbf{F}(\mathbf{y}(0), \dot{\mathbf{y}}(0)). \tag{87}$$

The Newton–Raphson method is used to compute $\mathbf{d}_{n+1}$, $\mathbf{v}_{n+1}$ and $\mathbf{a}_{n+1}$ with given Δt, $\mathbf{d}_n$, $\mathbf{v}_n$ and $\mathbf{a}_n$. To update the displacement and velocity in equations (78) and (79), $\mathbf{a}_{n+1}$ should be computed from equations (77)–(79). Substituting equations (78) and (79) into equation (77), the resultant equation becomes a non-linear algebraic vector equation for $\mathbf{a}_{n+1}$, if $\mathbf{d}_n$, $\mathbf{v}_n$ and $\mathbf{a}_n$ are known. This equation may be written as

$$\mathbf{G}(\mathbf{y}(\mathbf{a}_{n+1}), \dot{\mathbf{y}}(\mathbf{a}_{n+1}), \ddot{\mathbf{y}}(\mathbf{a}_{n+1})) = \mathbf{0}. \tag{88}$$

By applying the Newton–Raphson method, the updated acceleration $\mathbf{a}_{n+1}$ can be obtained from equation (88). The iteration procedure to solve equation (88) for $\mathbf{a}_{n+1}$ is given by

$$\mathbf{a}_{n+1}^{(j+1)} = \mathbf{a}_{n+1}^{(j)} + \Delta\mathbf{a}_{n+1}^{(j)}, \tag{89}$$

$$\mathbf{J}(\mathbf{a}_{n+1}^{(j)})\,\Delta\mathbf{a}_{n+1}^{(j)} = -\mathbf{G}(\mathbf{a}_{n+1}^{(j)}), \tag{90}$$

where j represents the iteration number for each time step and $\mathbf{J}(\mathbf{a}_{n+1}^{(j)})$ is the Jacobian matrix of $\mathbf{G}(\mathbf{a}_{n+1})$ at $\mathbf{a}_{n+1} = \mathbf{a}_{n+1}^{(j)}$ which may be expressed as

$$\mathbf{J}(\mathbf{a}_{n+1}^{(j)}) = \left[(1-\alpha_m)\frac{\partial \mathbf{G}}{\partial \ddot{\mathbf{y}}} + (1-\alpha_f)\,\gamma\Delta t\,\frac{\partial \mathbf{G}}{\partial \dot{\mathbf{y}}} + (1-\alpha_f)\,\beta\Delta t^2\,\frac{\partial \mathbf{G}}{\partial \mathbf{y}}\right]_{\mathbf{a}_{n+1}=\mathbf{a}_{n+1}^{(j)}}. \tag{91}$$

Time responses are computed for the stable regions I and II as well as the unstable region to verify the stability. The physical system parameters for computation are given by $M = 1\,\text{kg}$, $k = 1\times10^4\,\text{N/m}$, $c = 2\,\text{N s/m}$, $R = 0{\cdot}1\,\text{m}$, $\varepsilon = 1\times10^{-3}\,\text{m}$, $m = 0{\cdot}01\,\text{kg}$, $D = 1\times10^{-4}\,\text{N m/s}$. In this case, the natural frequency of the system is $\omega_n = 100\,\text{rad/s}$ and the corresponding non-dimensional

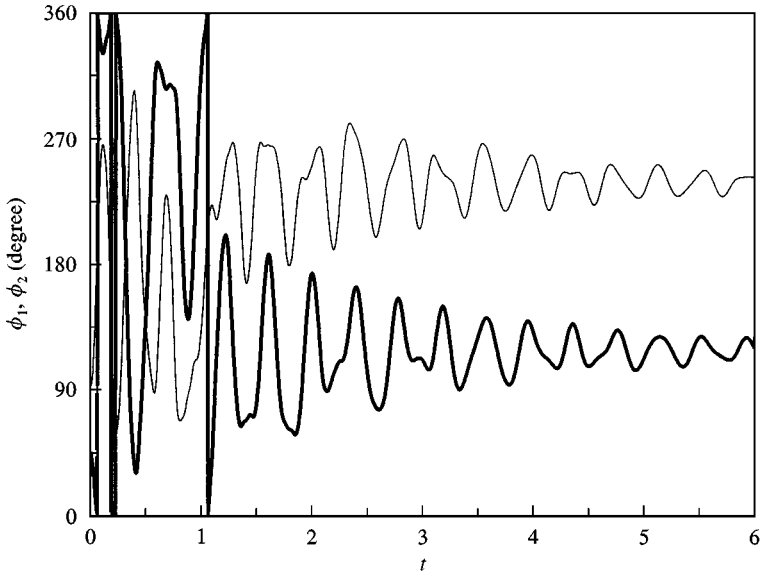

Figure 10. Time responses of the ball positions when $\omega/\omega_n = 2$ and $m/M = \varepsilon/R - \zeta = \bar{\beta} = 0{\cdot}01$

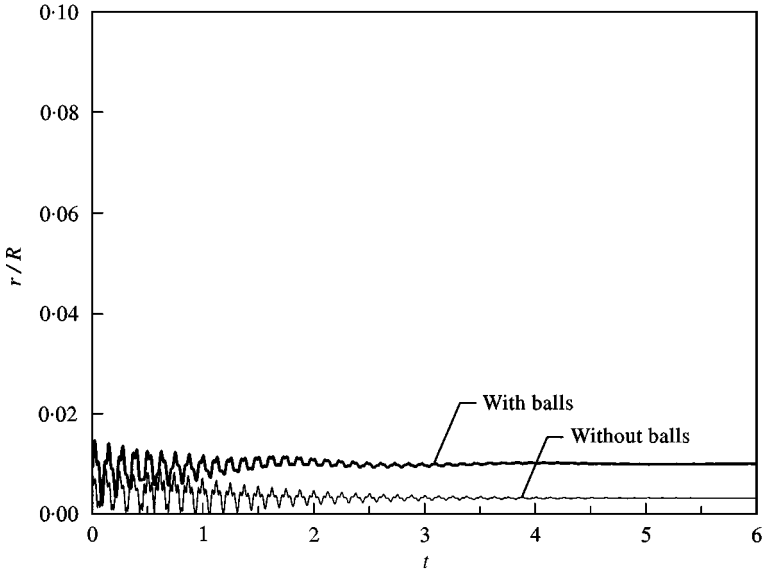

Figure 11. Time response of the radial displacement when $\omega/\omega_n = 0{\cdot}5$ and $m/M = \varepsilon/R = \zeta = \bar{\beta} = 0{\cdot}01$

parameters are $m/M = \varepsilon/R = \zeta = \dot{\bar{\beta}} = 0{\cdot}01$. The initial conditions are given by $r(0) = 1 \times 10^{-3}$ m, $\psi(0) = 0$, $\phi_1(0) = 45^\circ$, $\phi_1(0) = 90^\circ$ and $\dot{r}(0) = \dot{\psi}(0) = \dot{\phi}_1(0) = \dot{\phi}_2(0) = 0$. In the computation, $\Delta t = 5 \times 10^{-5}$ s and $\rho_\infty = 1$ are used. Note that the algorithmic parameter $\rho_\infty = 1$ implies that the generalized-α method does not have the numerical damping.

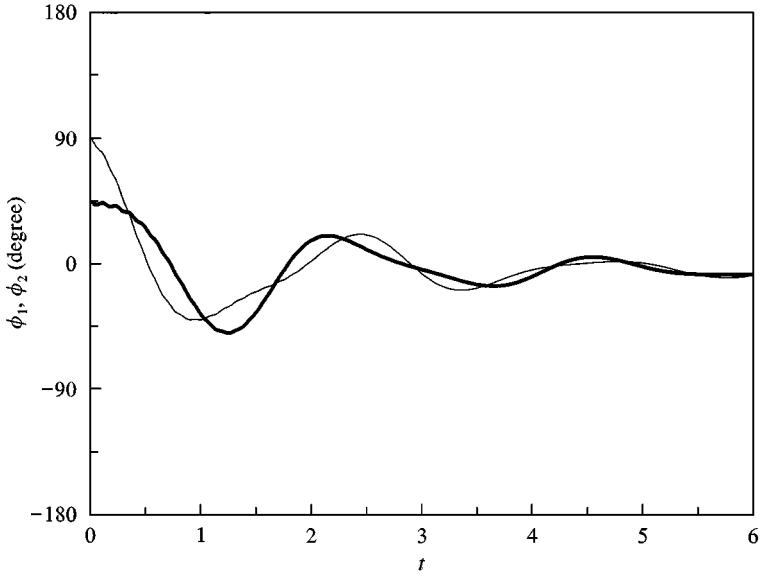

Figure 12. Time responses of the ball positions when $\omega/\omega_n = 0{\cdot}5$ and $m/M = \varepsilon/R = \zeta = \bar{\beta} = 0{\cdot}01$

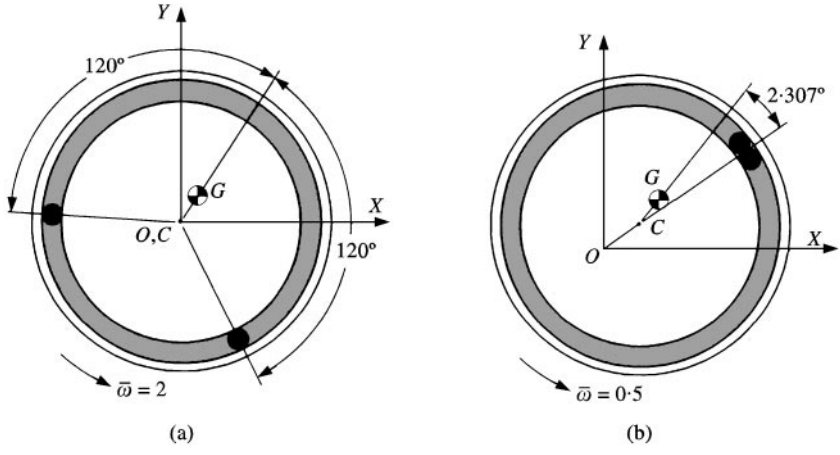

Figure 13. Position of the balls for (a) $\omega/\omega_n = 2$ and (b) $\omega/\omega_n = 0{\cdot}5$ When $m/M = \varepsilon/R = \zeta = \bar{\beta} = 0{\cdot}01$ and $t \to \infty$.

The time responses of the radial displacements and the ball positions are computed for $\omega/\omega_n = 2$, $\omega/\ \omega_n = 0{\cdot}5$ and $\omega/\omega_n = 1{\cdot}25$ which correspond to the stable region I, stable region II and unstable region respectively. In the stable region I, as shown in Figures 9 and 10, the radial displacement and the ball positions coverage to zero and constant values, respectively, as time increases. The converged ball positions are 120 and 240° which can be computed from equation (56). This means that the radial displacement and the ball positions approach the equilibrium positions corresponding to $r^* = 0$. Similarly, when $\omega/\omega_n = 0{\cdot}5$, i.e., when the system is in the stable region II, the radial displacement and the ball positions approach the equilibrium positions corresponding to $r^* \neq 0$, as illustrated in Figures 11 and 12. In this case, equations (70)–(72) provide

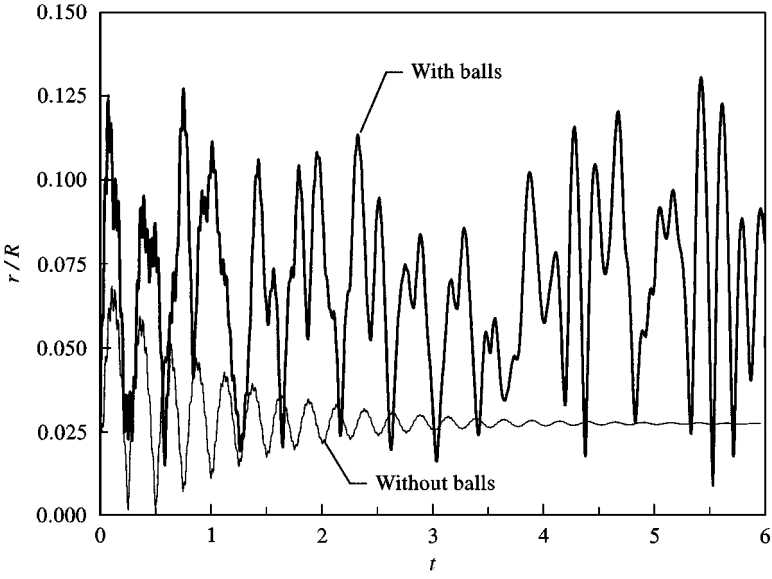

Figure 14. Time response of the radial displacement when $\omega/\omega_n = 1{\cdot}25$ and $m/M = \varepsilon/R = \zeta = \bar{\beta} = 0{\cdot}01$.

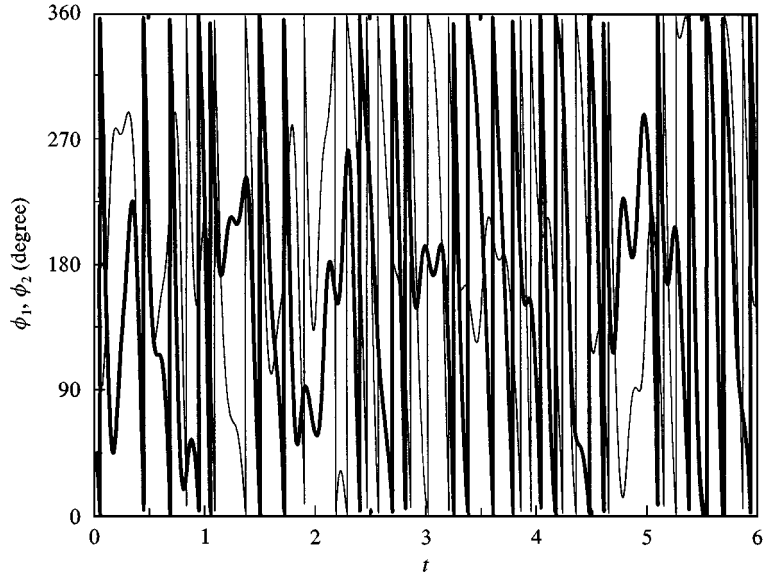

Figure 15. Time responses of the ball positions when $\omega/\omega_n = 1{\cdot}25$ and $m/M = \varepsilon/R = \zeta = \bar{\beta} = 0{\cdot}01$.

$r/R = 1{\cdot}006 \times 10^{-2}$ and $\phi_1 = \phi_2 = -2{\cdot}307^\circ$ when $t \to \infty$. The equal values of ϕ_1 and ϕ_1 implies that the balls are overlapped. Notice that the computation of this study neglects the impact and geometric interference between the balls. When the system is in the stable regions I and II, the ball psotions are plotted in (a) and (b) of Figure 13, respectively. Figure 13(a) shows that the rotor system is balance, i.e., point C coincides with point O if it is in the stable region I. However, when the system is in the stable region II, the balls are positioned in the direction of the mass

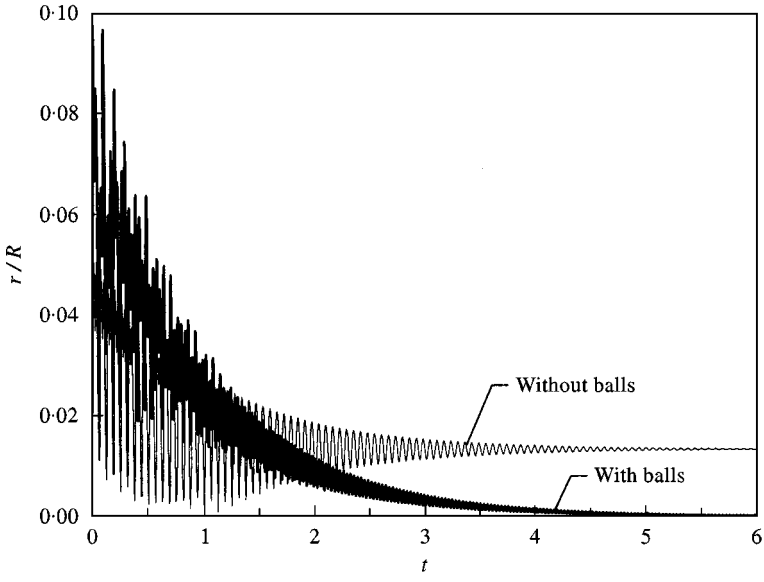

Figure 16. Time responses of the radial displacement when $\omega/\omega_n = 2$, $m/M_n = \varepsilon/R = \zeta = 0{\cdot}01$ and $\bar{\beta} = 0{\cdot}05$.

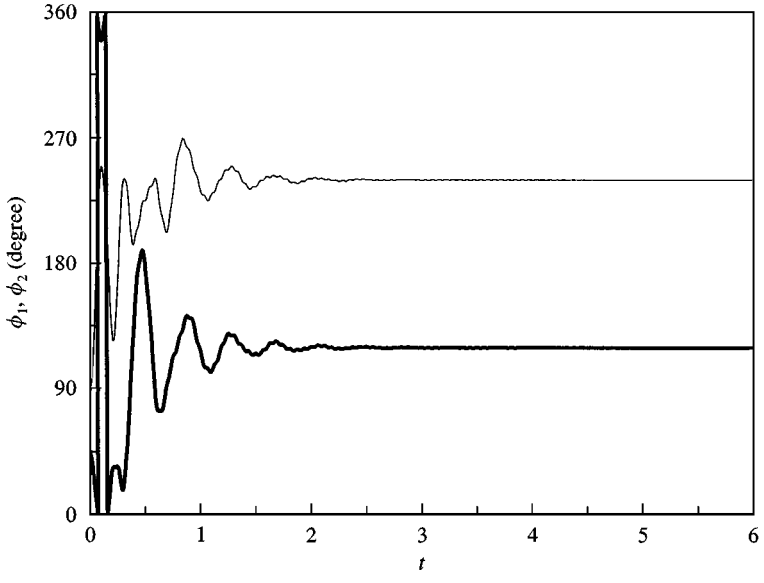

Figure 17. Time response of the ball positions when $\omega/\omega_n = 2$, $m/M = \varepsilon/R = \zeta = 0{\cdot}01$ and $\bar{\beta} = 0{\cdot}05$.

centre G, as exhibited in Figure 13(b). Therefore, the balls increase the total amount of unbalance for the system. On the other hand, if the system is in the unstable region, e.g., $\omega/\omega_n = 1{\cdot}25$, the radial displacement r and the ball positions, ϕ_1 and ϕ_2, do not have the converged values and they are varied continually with time, as shown in Figures 14 and 15.

Let us examine the effects of the fluid damping on the time responses when the system is balanced, namely, when $\omega/\omega_n = 2$ and $m/M = \varepsilon/R = \zeta = 0{\cdot}01$. In this case, the radial displacement and the ball positions are more rapidly converged to those of th equilibrium positions when $\bar{\beta} = 0{\cdot}05$ than when $\bar{\beta} = 0{\cdot}01$. Comparisons of Figures 16 and 17 with Figures 9 and 10 exhibits the fact that the fluid damping $\bar{\beta}$ is helpful for the system to obtain balancing.

6. CONCLUSIONS

The dynamic stability and time responses have been analyzed for the ADB. For the stability analysis, the non-linear equations of motion have been derived using the polar co-ordinate system instead of the rectangular co-ordinate system. It has been shown that the use of the polar co-ordinate system makes it possible to derive the equations of motion for the autonomous system, which are very efficient in order to analyze the stability.

Based on the equations for the autonomous system, the stability of the system have been systematically analyzed with the linear variational equations and the Routh–Hurwitz criteria. For the variations of the operating speed, damping factor, fluid damping, ball mass and eccentricity, this study investigates the dynamic states of the system that may be classified into the stable and unstable regions. It is shown that the stable regions are further divided into the balanced ($r^* = 0$) or unbalanced ($r^* \neq 0$) cases. In particular, the analysis demonstrates that the system may not achieve balancing even above the critical speed, i.e., $\omega/\omega_n > 1$. Hence, it is expected that the analysis results provide design requirements for the physical parameters of a system so that an ADB can obtain balancing. On the other hand, the analysis for the time responses shows that the system reaches the equilibrium positions with time when it is in the stable regions. In addition, it is also shown that the fluid damping $\bar{\beta}$ is helpful for the ADB to obtain balancing.

ACKNOWLEDGMENT

The authors would like to acknolwedge the support provided by the ROM Business Team of Samsung Electronics Co., Ltd.

REFERENCES

1. J. D. Alexander 1964 *Proceedings for the Second Southeastern Conference* **2**, 415–426. An automatic dynamic balancer.
2. J. W. Cade 1965 *Design News*, 234–239. Self-compensating balancing in rotating mechanisms.
3. J. Lee 1995 *Shock and Vibration* **2**, 59–67. An analytical study of self-compensating dynamic balancer with damping fluid and ball.
4. J. Lee and W. K. Van Moorhem 1996 *ASME Journal of Dynamic Systems, Measurement, and Control* **118**, 468–475. Analytical and experimental analysis of a self-compensating dynamic balancer in a rotating mechanism.
5. J. Chung and G. M. Hulbert 1993 *ASME Journal of Aplied Mechanics* **60**, 371–375. A time integration algorithm for structural dynamics with improved numerical dissipation: the generalized-α method.